Transactions on Additive Manufacturing Meets Medicine
Trans. AMMM, Vol. 4, No 1, Article ID 674, 4 Pages

Infinite Science Publishing

Original Research Article

Experimental FSI simulation validation of an anthropomorphic upper airway phantom

A. Ibbeken[1*], F. Zell[1*], C. Hagen[1], U. Grzyska[2], A. Frydrychowicz[2], A. Steffen[3], and T. M. Buzug[1,4]

[1] *Institute of Medical Engineering, Universität zu Lübeck, Lübeck, Germany*

[2] *Department of Radiology and Nuclear Medicine, Universität zu Lübeck, Lübeck, Germany*

[3] *Department of Otolaryngology, Universität zu Lübeck, Lübeck, Germany*

[4] *Fraunhofer Research Institution for Individualized and Cell-Based Medical Engineering IMTE, Lübeck, Germany*

[*] *Corresponding author, email: ibbeken@imt.uni-luebeck.de zell@imt.uni-luebeck.de*

Abstract: Obstructive sleep apnea (OSA) is a common sleeping disorder characterized by the reversible partial or complete obstruction of the upper airway during sleep. Simulating airflow and resulting soft tissue deformations in the upper airway can help to understand the causes that lead to OSA and help to improve therapy options. In this work, the interaction between airflow and the surrounding soft tissue of an upper airway model including the nasal structures was examined with a fluid-structure interaction (FSI) in-silico simulation. The simulation was validated with experimental measurements. An anthropomorphic 3D printed upper airway phantom of an obstructive sleep apnea patient was fabricated and used in deformation measurements to reproduce an inhalation process with a maximal flow rate of 15 l/min. The deformation was measured with a CT scanner and compared to the corresponding FSI simulation results. The comparison showed good agreement in the resulting deformation.

I. Introduction

Obstructive sleep apnea is a common sleep-related disorder characterized by episodic partial or complete collapses of the upper airway due to a shift of the surrounding soft tissue. Mostly, the collapse occurs in the retropalatal or oropharyngeal area in 56-75 % of OSA patients [1]. Due to severe comorbidities and secondary diseases like cardio-vascular diseases, diabetes, depression and excessive daytime sleepiness a proper treatment of OSA is highly recommended [2]. FSI simulations of airflow and resulting deformation can help to gain a higher understanding of patient specific processes. In this work, we present an FSI simulation of an upper airway of an OSA patient, that was validated with deformation measurements with a 3D printed and silicone casted upper airway model.

II. Material and methods

A flexible anthropomorphic airway phantom was fabricated to perform flow dependent deformation measurements. The measurements were used to validate FSI simulations.

II.I. Model fabrication and deformation measurements

MR images (3T Philips Ingenia, 3D T1 TSE sequence) of the upper airway including the nasal structures of a 56-year-old female OSA patient with a BMI of 36 were used as data basis. The patient has a two nights-averaged apnea-hypopnea-index (AHI) of 27 and an oxygen desaturation index (ODI) of 15 indicating moderate OSA. Healthy people have an AHI below 5 and ODI less than 10.

The model was fabricated using additive manufacturing and silicone casting techniques. Therefore the soft tissue components were merged together and produced with silicone Sylgard 527 (Sylgard 527 Silicone Elastomere, Dow Corning, Midland, Michigan, USA) using the 3D printed casting mould. Sylgard 527 has a Youngs modulus of 5 kPa [3] which according to [4] and [5] is in the same range as the upper airway elastic tissue. The airway structure was printed with water-soluble material (Premium PLA filament and Atlas PVA filament, FormFutura, Nijmegen, The Netherlands) and removed in a water bath after soft tissue fabrication was completed.

Infinite Science Publishing

For more information about the preprocessing and fabrication process of the hardware phantom see [6]. Fig. 1 shows the comparison between the MR images of the upper airway of the OSA patient and the corresponding fabricated hardware phantom. The computer-aided design of the upper airway phantom, the water-soluble pharynx, and the measurement setup in the CT scanner are shown in Fig. 2.

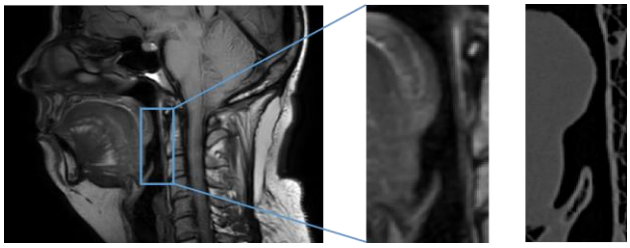

Figure 1: MR image of the upper airway of an OSA patient (left) and corresponding 3D printed upper airway phantom (right).

For CT deformation measurements a flow rate of 15 l/min steady airflow was used mimicking physiological inspirational behavior during quite breathing [7].

A reference measurement with no applied flow was taken. Airflow was acquired using a custom-made flow pump. For flow measurements a mass flow meter from Sensirion (SFM 3000, Sensirion, Stäfa, Switzerland) was used.

The CT images were acquired with a Siemens CT scanner (Somatom Definition AS+, Siemens Healthineers, Erlangen, Germany) with a voxel spacing of 0.4 x 0.4 x 0.3 mm^3 and a peak tube voltage of 120 kVp.

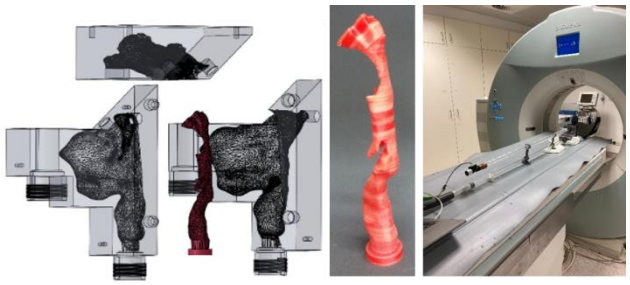

Figure 2: Explosion view of the casting mold with integrated soft tissue and water-soluble airway (left), 3D printed water-soluble airway (middle) and measurement setup in the CT scanner (right).

The segmentation of the upper airway was performed with Mimics (Materialise Mimics, Materialise NV, Leuven, Belgium) with automatic threshold segmentation.

For determining the deformation, the deformed model was compared to the undeformed reference model by calculating the least distance between the models for every node of the segmented STL files. Besides the no flow reference measurement that was conducted prior to the deformation measurement, a second no flow measurement was performed afterwards, to examine the elastic behavior of the silicone restoring its original shape.

II.II. Simulation setup and boundary conditions

The digital airway model created to print the hardware phantom was also used for the FSI simulation. For this purpose, the simulation software COMSOL Multiphysics 6.0 (COMSOL Multiphysics GmbH, Göttingen, Germany) is used. The airway and surrounding soft tissue, like the tongue and the soft palate were considered in the simulation, whereas the surrounding rigid casting mold of the hardware model and the fixed tissue around the nasal structures were neglected to reduce computational cost. The digital model is shown in Fig 3 (left).

For the simulation of airflow through the airway, the fluid can be considered as incompressible, due to the low velocity that occurs during inhalation (Mach number MA < 0.05). The Reynolds number (Re) was estimated in a laminar region for a maximum flow rate of 15 l/min, which was the flow rate in the experimental setup. To simulate the behavior of the fluid, the incompressible Navier-Stokes equations are used. They describe the conservation law of mass and momentum

$$\nabla \boldsymbol{u} = \boldsymbol{0} \tag{1}$$

$$\frac{\partial \boldsymbol{u}}{\partial t} + \boldsymbol{u} \cdot \nabla \boldsymbol{u} - \mu \Delta \boldsymbol{u} + \frac{1}{\rho} \nabla \boldsymbol{p} = \boldsymbol{g} \tag{2}$$

where $\boldsymbol{u}$ is the velocity vector, p pressure, $\boldsymbol{g}$ external forces, μ dynamic viscosity of air ($\mu = 1.814 \cdot 10^{-5}$ Pa·s) and its density with $\rho = 1.204\ kg/m^3$

The basic equations of continuum mechanics, which mathematically describe the behavior of a structure, are modeled by the kinematic relations and the material law. The surrounding soft tissue modeled in the hardware phantom with the silicone Sylgard 527, can be considered as hyper-elastic. Therefore, a Youngs modulus of E = 5000 Pa, Poisson's ratio $\nu = 0.49$ and a density of $\rho = 1032\ kg/m^3$ were chosen as material parameters.

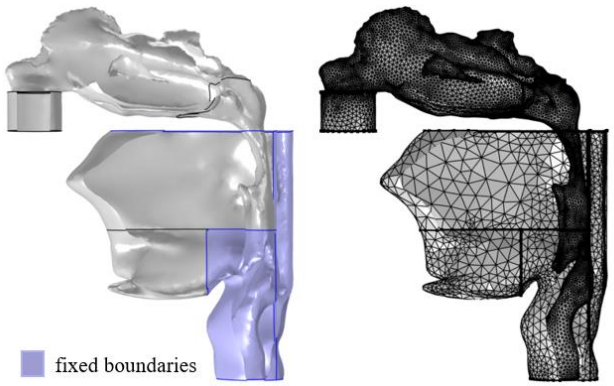

Figure 3: Digital model of the phantom for FSI simulation, where the purple boundaries are considered to be fixed (left) and the computational mesh with 371,284 elements, which is composed of tetrahedral (278,560), pyramidal (706) and prismatic (92,018) elements (right).

Infinite Science Publishing

To simulate flow with a flow rate $\dot{V}$ as in the experimental setup, a velocity $\boldsymbol{u} = \dot{V}/A\,\boldsymbol{n}$ is defined at the outlet of the trachea, where $\dot{V} = 15\ l/min$ and were A is defined as the area of the outlet with normal vector $\boldsymbol{n}$. The velocity increases constantly until the maximum flow rate has been reached after 1 s to improve convergence. At the inlet a relative pressure of 0 Pa is selected as boundary condition.

To ensure that the degrees of freedom of the deformation were similar to the phantom, the areas around the epiglottis and trachea were defined as fixed (see Fig. 3, purple areas). Otherwise, large deformations would occur in the area of the fixed trachea, which is not realistic due to the cartilaginous structure of the trachea and was not observed in the deformation measurements. In addition, the posterior wall of the soft tissue was also assumed to be fixed, as the phantom has significantly less soft tissue in this area due to the fabrication of the model. In addition, the movement of the soft tissue is limited here by the vertebral bones.

In COMSOL Multiphysics, the discretization is based on the finite element method. The computational mesh was automatically created in COMSOL based on applied physics and consists of 371,284 elements, which is composed of tetrahedral (278,560), pyramidal (706), and prismatic (92,018) elements. The average element quality related to the equiangular skewness is 0.63, where 0 represents a degenerate element with large or small angles compared to the angles in an ideal element and 1 represents the best possible element. The mesh is shown in Fig. 3 (right).

For the time-dependent FSI simulation, the conservation equations for the fluid domain and the structure domain are solved by a fully coupled solver.

The FSI simulation was obtained on a cluster (4x Intel Xeon E5-4657L v2 @ 2.40 GHz, 1 TB RAM) which demanded 18.56 GB memory and a computation time of 6 h 20 min.

III. Results and discussion

Fig. 4 shows the resulting deformation of the measurement (left) in comparison to the calculated deformation from the simulation (right) in mm. Here, the retropalatal region, which is defined from the beginning of the oropharynx (z = 0 mm) – which will be referred to as pharyngeal inlet -to the tip of the epiglottis (z = 50 mm), was considered. In the measurement, a maximum deformation in the retropalatal region of approximately 0.4 mm is observed and 0.35 mm in the simulation. Due to the small deformations, which are below the CT resolution (i.e. less than 0.4 mm^3), it cannot be concluded that the simulations and measurements agree in quantity. But, the regions of deformation are in good agreement. In the region, which corresponds to the area behind the tongue, the phantom contracts due to flow forces in the simulation as well as in the measurement. At the inlet of the phantom a slightly different deformation behavior appears. While in the simulation no deformation is occurring in this area, in the measurements a slight expansion of the phantom of approximately 0.2 mm can be observed. Due to the low resolution of the CT measurement the accuracy of the that deformation cannot be appraised without further measurements.

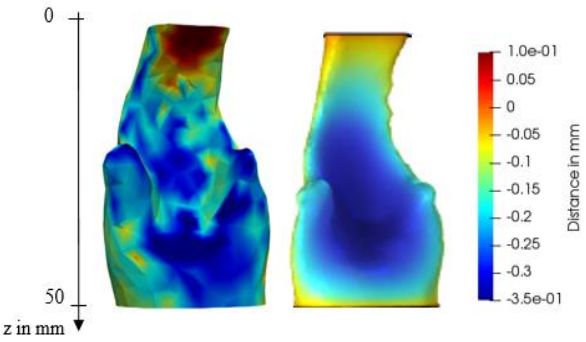

Figure 4: Comparison of the resulting deformation of the measurement (left) and the simulation (right) in the retropalatal region in mm. The region is defined from the beginning of the oropharynx (z = 0 mm) to the tip of the epiglottis (z = 50 mm).

The comparison of the deformation behavior along the midline is depicted in Fig. 5. Here the deviation between measurement and simulation can be seen at the boundaries to the pharyngeal inlet (z=0 mm) and to the epiglottis (z=50 mm), due to the predefined fixed planes which limit the deformation of the simulation.

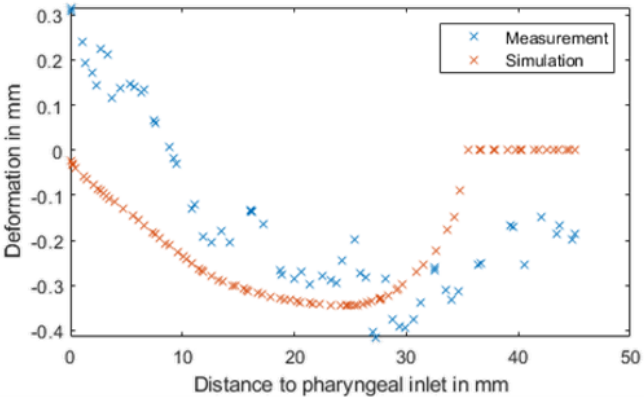

Figure 5: Comparison of the simulated and measured deformation along the midline of the retropalatal region of the phantom. The resolution of the CT measurement is 0.3 x 0.3 x 0.4 mm^3 *and is thus below the deformations that occur.*

By comparing the no flow measurements that were acquired before deformation and after deformation it has been verified that the silicone representing the upper airway soft tissue returns to its original shape and thus can be used for further measurements.

Due to the narrowing of the pharynx in the retropalatal region, a velocity jet with a maximum velocity of 14.6 m/s is developed (see Fig. 6). The jet is shifted to the left side, where a pressure drop occurs. The pressure distribution over the entire model is shown in Fig. 7. The pressure drop

occurs at the front side of the pharynx, where the movable soft tissue is located. To achieve a flow rate of 15 l/min a mean pressure of -178 Pa is required at the outlet.

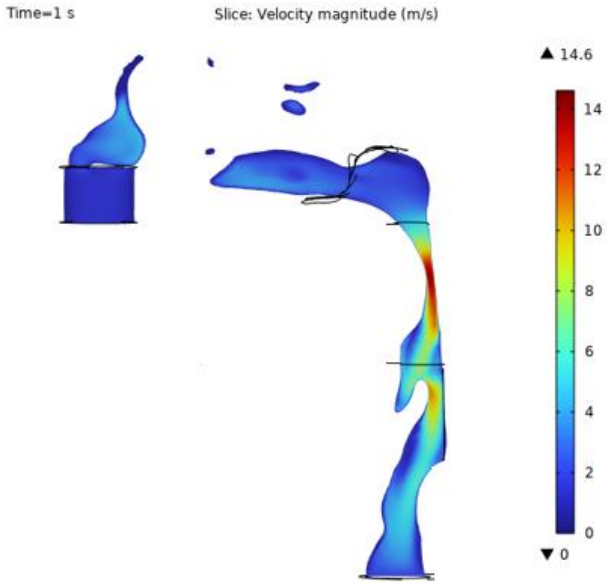

Figure 6: Cross-section through the model showing flow velocities in m/s. A jet with a maximum velocity of 14.6 m/s is developed.

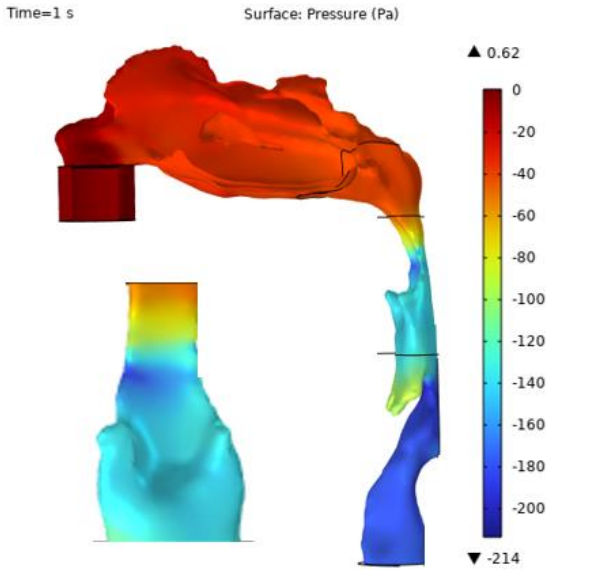

Figure 7: Simulated pressure distribution in Pa. A pressure of 0 Pa is specified as a boundary condition at the inlet. A pressure drop occurs at the front side of the pharynx.

IV. Conclusions

All in all measurements and simulations have shown that at a flow rate of 15 l/min small deformations occur in the upper airway, especially in the retropalatal region. The deformations that occur are below the resolution of the CT used, so that a quantitative comparison of the deformations between simulations and measurements is not possible.

However, it could be shown that the region of the occurring deformations agrees. Slight deviations in the behavior of the deformation occur at the inlet of the phantom. Deformation measurements with a higher resolution have to be performed to compare the results.

To achieve even better correspondence fixed boundary conditions at the regions of the inlet, trachea and epiglottis of the simulation can be adapted. Instead of predefining the fixed boundaries with simple planes, the area should be defined precise using anatomical segmentation of the trachea and epiglottis. In addition, an explanation for the slight deviance might be the production-related deviation of the hardware model from the original segmentation of the upper airway geometry (for more information see [6]). Therefore, the redigitized model from the CT deformation measurements without flow could be used to minimize deviations between simulation and experimental model. To gain even more measurement parameters to validate the simulation a corresponding hardware flow phantom with integrated pressure sensors is being planned. CT measurements with a higher resolution are planned in the future to reproduce the validation with a more accurate resolution suitable for the low measuring range.

Acknowledgments

This work has been funded by the German Federal Ministry of Education and Research (BMBF Grant Number 13GW0276B).

Author's Statement

Authors state no conflict of interest. Informed consent: Informed consent has been obtained from all individuals included in this study. Ethical approval: The research related to human use complies with all the relevant national regulations, institutional policies and was performed in accordance with the tenets of the Helsinki Declaration, and has been approved by the authors' institutional review board or equivalent committee.

References

[1] C. M. Rayn, T. D. Bradley, *Pathogenesis of obstructive sleep apnea*, Journal of Applied Physiology, Vol 99 No 6, pp. 2440-2450, 2005.

[2] American Academy of Sleep Medicine, I*nternational classification of sleep disorders, revised: Diagnostic and coding manual*, American Academy of Sleep Medicine, 2001.

[3] R.N. Palchelsko, L. Zhang, Y. Sun, A.W. Feinberg, *Development of Polydimethylsiloxane substrates with Tunable Elastic Modulus to Study Cell Mechanobiology in Muscle and Nerve*, PLoS ONE 7(12): e51499, 2012.

[4] A. Malhotra, Y. Huang, R.B. Fogel, G. Pillar, J.K. Edwards, R. Kikinis, S.H. Loring, D.P. White, *The Male Predisposition to Pharyngeal Collapse Importance of Airway Length*, American Journal of Respiratory and Critical Care Medicine, vol. 166, pp. 1388-1395, 2002.

[5] S. Cheng, S.C. Gandecia, M. Green, R. Sinkus, L.E. Bilston, *Viscoelastic properties of the tongue and soft palate using MR elastography*, Journal of biomechanics. 44(3):450-4, 2011.

[6] A. Ibbeken, C. Hagen, F. Zell, A. Steffen, U. Grzyska, A. Frydrychowicz, T.M. Buzug, *Design and construction of a flexible pharyngeal phantom*, Transactions on Additive Manufacturing Meets Medicine, Vol 3 No 1, 2021.

[7] M. Rahimi-Gorji, O. Pourmehran, M. Gorji-Bandpy, T.B. Gorji, *CFD simulation of airflow behavior and particle transport and deposition in different breathing conditions through the realistic model of human airways*, Journal of Molecular Liquids, vol. 209, pp. 121-133, 2015.